

Transmit Antenna Selection with Alamouti Scheme in MIMO Wiretap Channels

Shihao Yan, Nan Yang, Robert Malaney, and Jinhong Yuan

School of Electrical Engineering and Telecommunications, The University of New South Wales, Sydney, NSW, Australia

Email: shihao.yan@student.unsw.edu.au, nan.yang@unsw.edu.au, r.malaney@unsw.edu.au, j.yuan@unsw.edu.au

Abstract—This paper proposes a new transmit antenna selection (TAS) scheme which provides enhanced physical layer security in multiple-input multiple-output (MIMO) wiretap channels. The practical passive eavesdropping scenario we consider is where channel state information (CSI) from the eavesdropper is not available at the transmitter. Our new scheme is carried out in two steps. First, the transmitter selects the first two strongest antennas based on the feedback from the receiver, which maximizes the instantaneous signal-to-noise ratio (SNR) of the transmitter-receiver channel. Second, the Alamouti scheme is employed at the selected antennas in order to perform data transmission. At the receiver and the eavesdropper, maximal-ratio combining is applied in order to exploit the multiple antennas. We derive a new closed-form expression for the secrecy outage probability in non-identical Rayleigh fading, and using this result, we then present the probability of non-zero secrecy capacity in closed form and the ε -outage secrecy capacity in numerical form. We demonstrate that our proposed TAS-Alamouti scheme offers lower secrecy outage probability than a single TAS scheme when the SNR of the transmitter-receiver channel is above a specific value.

I. INTRODUCTION

Physical layer security in wireless communication networks has recently gained considerable research interest [1]. The core concept behind this paradigm is to exploit the properties of a wireless channel, such as fading or noise, to promote secrecy for wireless transmission [2]. Physical layer security, in principle, eliminates the requirement for complex higher-layer secrecy techniques, such as encryption and cryptographic key management. In early pioneering studies [3–5], the wiretap channel was characterized as the fundamental framework within which to protect information at the physical layer. In the wiretap channel where the transmitter (commonly known as Alice), the receiver (Bob) and the eavesdropper (Eve) are equipped with a single antenna, it was proved that perfect secrecy can be achieved if the eavesdropper's channel between Alice and Eve is worse than the main channel between Alice and Bob. Motivated by emerging multiple-input multiple-output (MIMO) techniques, there is a growing interest in investigating the MIMO wiretap channel [6, 7]. In the MIMO wiretap channel where Alice, Bob, and/or Eve are equipped with multiple antennas, it was established that the perfect secrecy can be guaranteed via beamforming with/without artificial noise even if the quality of the eavesdropper's channel is higher than that of the main channel [8, 9].

When the CSI of the eavesdropper's channel is not available at Alice, perfect secrecy can not be guaranteed. In this circumstance, the secrecy performance is investigated from

the perspective of wireless channel statistics. Correspondingly, secrecy outage probability is adopted as a practical and important performance metric to evaluate the probability that the actual transmission rate is larger than the instantaneous secrecy capacity [10]. To avoid the high feedback overhead and high signal processing cost required by beamforming, transmit antenna selection (TAS) was proposed to enhance physical layer security in MIMO wiretap channels [11, 12]. In this TAS scheme, only one antenna is selected at Alice to maximize the instantaneous signal-to-noise ratio (SNR) of the main channel. Throughout this paper, we refer to this scheme as *single TAS*. Single TAS significantly reduces the feedback overhead and hardware complexity, since only the index of the selected transmit antenna is fed back from the receiver and only one radio-frequency chain is implemented at the transmitter. Motivated by this, [11] derived the secrecy outage probability of single TAS for the wiretap channel with multiple antennas at Alice and Eve but a single antenna at Bob. A general wiretap channel model with multiple antennas at Alice, Bob, and Eve was investigated in [12], in which the performance of single TAS with maximal-ratio combining (MRC) or selection combining (SC) was thoroughly examined in Rayleigh fading. Considering versatile Nakagami- m fading, [13] analyzed the secrecy performance of single TAS.

In general, the practicality of TAS schemes is determined by not only the achievable performance but the incurred feedback overhead and hardware complexity. As such, it is possible to select more than one antenna at the transmitter for transmission. For such multi-antenna selection schemes, effective coding strategies need to be incorporated according to the number of selected antennas [14]. A practical example is the Alamouti scheme which offers full diversity order [15]. Against this background, [16] proposed a new TAS-Alamouti scheme in MIMO systems without secrecy constraints. In this scheme, two transmit antennas are selected at the transmitter and the Alamouti scheme is adopted to perform data transmission through the selected antennas. Notably, it was observed in [16] that the performance of TAS-Alamouti is worse than that of single TAS in MIMO systems without secrecy constraints. The reason for this observation lies in the fact that TAS-Alamouti wastes transmit energy on the second selected antenna.

In this paper, we examine the interesting questions: “*Is the secrecy performance in MIMO wiretap channels improved if two antennas are selected at the transmitter instead of one?*”

And if so, by how much?” In order to address this question, we propose TAS-Alamouti in MIMO wiretap channels to enhance physical layer security. In this MIMO wiretap channel, Alice, Bob, and Eve are equipped with N_A , N_B , and N_E antennas, respectively. In our proposed TAS-Alamouti scheme, the first two strongest transmit antennas are selected at Alice and the Alamouti scheme is applied at the two selected antennas to carry out data transmission. At Bob and Eve, MRC is applied to combine the received signals. To quantify the performance of our scheme, we derive a new closed-form expression for the secrecy outage probability. Based on this result, we characterize the probability of non-zero secrecy capacity and ε -outage secrecy capacity. Our key conclusion is that our proposed TAS-Alamouti scheme achieves a lower secrecy outage probability than the single TAS scheme when the SNR of the main channel is in the medium and high regime relative to the SNR of the eavesdropper’s channel. This useful result is quite a surprising given the previous studies of similar schemes in MIMO systems without secrecy constraints [16].

The rest of this paper is organized as follows. Section II details the system model and the proposed TAS-Alamouti scheme. In Section III, the secrecy performance of the proposed TAS-Alamouti scheme is analyzed. Numerical results are presented in Section IV. Finally, Section V draws some concluding remarks and future directions.

Notation: Scalar variables are denoted by italic symbols. Vectors and matrices are denoted by lower-case and upper-case boldface symbols, respectively. Given a complex vector \mathbf{x} , $\|\mathbf{x}\|$ denotes the Euclidean norm, $(\mathbf{x})^T$ denotes the transpose operation, and $(\mathbf{x})^\dagger$ denotes the conjugate transpose operation. The $m \times m$ identity matrix is referred to as \mathbf{I}_m .

II. SYSTEM MODEL AND PROPOSED TAS-ALAMOUTI

Fig. 1 depicts the MIMO wiretap channel of interest, where the transmitter (Alice), the receiver (Bob), and the eavesdropper (Eve) are equipped with N_A , N_B , and N_E antennas, respectively. We assume that the main channel between Alice and Bob and the eavesdropper’s channel between Alice and Eve are subject to quasi-static Rayleigh fading. Under this assumption, the fading coefficients are invariant during two adjacent blocks of time durations within which the Alamouti scheme is applied. We also assume the same fading block length in the main channel and the eavesdropper’s channel. For such a wiretap channel, the passive eavesdropping scenario is considered where Eve overhears the transmission between Alice and Bob without inducing any interference to the main channel. In this scenario, the instantaneous channel state information (CSI) of the eavesdropper’s channel is not available at Alice. Of course, we preserve the assumption that Bob has the full CSI of the main channel and Eve has the full CSI of the eavesdropper’s channel.

We propose a TAS-Alamouti scheme to enhance the physical layer security in the MIMO wiretap channel of interest. Specifically, the proposed scheme is performed in two steps. We next detail the two steps, as follows:

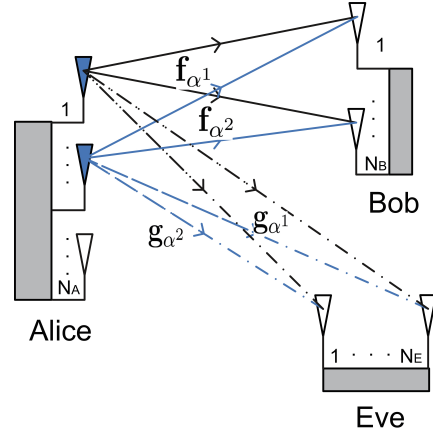


Fig. 1. Illustration of a MIMO wiretap channel with N_A , N_B , and N_E antennas at Alice, Bob, and Eve, respectively.

1) *First Step – TAS:* In the first step, the first two strongest antennas out of N_A antennas are selected at Alice. These two antennas maximize the instantaneous SNR between Alice and Bob. Here, Bob employs MRC to combine the received signals. As per this criterion, the index of the first strongest antenna is given by

$$\alpha_1 = \underset{0 \leq \alpha \leq N_A}{\operatorname{argmax}} \|\mathbf{f}_\alpha\| \quad (1)$$

and the index of the second strongest antenna is given by

$$\alpha_2 = \underset{0 \leq \alpha \leq N_A, \alpha \neq \alpha_1}{\operatorname{argmax}} \|\mathbf{f}_\alpha\|. \quad (2)$$

In (1) and (2), we denote $\mathbf{f}_\alpha = [f_{\alpha,1}, f_{\alpha,2}, \dots, f_{\alpha,N_B}]^T$ as the $N_B \times 1$ channel vector between the α -th antenna at Alice and the N_B antennas at Bob with independent and identically distributed (i.i.d.) Rayleigh fading entries.

To conduct antenna selection, Alice sends Bob pilot symbols prior to data transmission. Using these symbols, Bob precisely estimates the CSI of the main channel and determines α_1 and α_2 according to (1) and (2). After that, Bob feeds back α_1 and α_2 to Alice via a low-rate feedback channel. As such, our scheme reduces the feedback overhead compared with beamforming, since only a small number of bits are required to feedback the antenna indices. We note that the antenna indices (1) and (2) are entirely dependent on the main channel. As such, the two strongest transmit antennas for Bob corresponds to two random transmit antennas for Eve. It follows that our scheme improves the quality of main channel relative to the eavesdropper’s channel, which in turn promotes the secrecy of the wiretap channel.

2) *Second Step – Alamouti:* In the second step, Alice adopts the Alamouti scheme to perform secure transmission at the two selected antennas. After receiving the signals from Alice, Bob applies MRC to combine the received signals and maximize the SNR of the main channel. This allows Bob to exploit the N_B -antenna diversity and maximize the probability of secure transmission. At the same time, Eve applies MRC to exploit

the N_E -antenna diversity and maximize the probability of successful eavesdropping.

As per the rules of the Alamouti scheme, the received signal vectors at Bob in the first and second time slots are given by

$$\mathbf{y}_B(1) = [\mathbf{f}_{\alpha_1}, \mathbf{f}_{\alpha_2}] \begin{bmatrix} x_1 \\ x_2 \end{bmatrix} + \mathbf{n}(1), \quad (3)$$

and

$$\mathbf{y}_B(2) = [\mathbf{f}_{\alpha_1}, \mathbf{f}_{\alpha_2}] \begin{bmatrix} -x_2^\dagger \\ x_1^\dagger \end{bmatrix} + \mathbf{n}(2), \quad (4)$$

respectively, where $[\mathbf{f}_{\alpha_1}, \mathbf{f}_{\alpha_2}]$ is the $N_B \times 2$ main channel matrix after TAS, $[x_1, x_2]^T$ is the transmit signal vectors in the first time slot, $[-x_2^\dagger, x_1^\dagger]^T$ is the transmit signal vectors in the second time slot, and \mathbf{n} is the zero-mean circularly symmetric complex Gaussian noise vector satisfying $\mathbb{E}[\mathbf{n}\mathbf{n}^\dagger] = \mathbf{I}_{N_B}\sigma^2$. Under the power constraint, we have $\mathbb{E}[|x_1|^2] = \mathbb{E}[|x_2|^2] \leq P_A/2$, where P_A is the total transmit power at Alice.

By performing MRC and space-time signal processing, the signals at Bob are expressed as

$$\mathbf{y}_B^1 = (\mathbf{f}_{\alpha_1}^\dagger \mathbf{f}_{\alpha_1} + \mathbf{f}_{\alpha_2}^\dagger \mathbf{f}_{\alpha_2}) x_1 + \mathbf{f}_{\alpha_1}^\dagger \mathbf{n}(1) + \mathbf{n}(2)^\dagger \mathbf{f}_{\alpha_2}, \quad (5)$$

and

$$\mathbf{y}_B^2 = (\mathbf{f}_{\alpha_1}^\dagger \mathbf{f}_{\alpha_1} + \mathbf{f}_{\alpha_2}^\dagger \mathbf{f}_{\alpha_2}) x_2 + \mathbf{f}_{\alpha_2}^\dagger \mathbf{n}(1) - \mathbf{n}(2)^\dagger \mathbf{f}_{\alpha_1}. \quad (6)$$

Since $\mathbf{n}(1)$ and $\mathbf{n}(2)$ are independent from each other, the instantaneous SNR at Bob for x_1 is identical to the instantaneous SNR at Bob for x_2 , which is written as

$$\gamma_B = \frac{(\|\mathbf{f}_{\alpha_1}\|^2 + \|\mathbf{f}_{\alpha_2}\|^2)P_A}{2\sigma^2}. \quad (7)$$

Following the same procedure as detailed above, the instantaneous SNR at Eve is written as

$$\gamma_E = \frac{(\|\mathbf{g}_{\alpha_1}\|^2 + \|\mathbf{g}_{\alpha_2}\|^2)P_A}{2\sigma^2}, \quad (8)$$

where $[\mathbf{g}_{\alpha_1}, \mathbf{g}_{\alpha_2}]$ is the $N_E \times 2$ eavesdropper's channel matrix after TAS and $\mathbf{g}_\alpha = [g_{\alpha,1}, g_{\alpha,2}, \dots, g_{\alpha,N_E}]^T$ denotes the $N_E \times 1$ channel vector between the α -th antenna at Alice and the N_E antennas at Eve with i.i.d. Rayleigh fading entries.

III. SECRECY PERFORMANCE OF TAS-ALAMOUTI

In this section, we concentrate on the secrecy performance of the proposed TAS-Alamouti scheme for non-identical Rayleigh fading between the main channel and the eavesdropper's channel. Specifically, we derive a new closed-form expression for the secrecy outage probability. Based on this result, we express the probability of non-zero secrecy capacity in closed form and present the ε -outage secrecy capacity in integral form.

A. Secrecy Outage Probability

The secrecy outage probability is defined as the probability of the secrecy capacity C_s being less than a specific transmission rate R_s (bits/channel) [10]. In the MIMO wiretap channel, C_s is expressed as

$$C_s = \begin{cases} C_B - C_E & , \quad \gamma_B > \gamma_E \\ 0 & , \quad \gamma_B \leq \gamma_E, \end{cases} \quad (9)$$

where $C_B = \log_2(1 + \gamma_B)$ is the capacity of the main channel and $C_E = \log_2(1 + \gamma_E)$ is the capacity of the eavesdropper's channel. Here, γ_B is the instantaneous SNR at Bob given by (7) and γ_E is the instantaneous SNR at Eve given by (8). According to the definition, the secrecy outage probability is formulated as

$$P_{out}(R_s) = \Pr(C_s < R_s). \quad (10)$$

We commence our analysis by presenting the probability density functions (pdfs) of γ_B and γ_E . Specifically, we adopt [16, Eq. (15)] as the pdf of γ_B , $f_{\gamma_B}(\gamma)$, and define $\bar{\gamma}_B$ as the average per-antenna SNR at Bob. We note that α_1 and α_2 are equivalent to two random transmit antennas for Eve. As such, the pdf of γ_E , $f_{\gamma_E}(\gamma)$, is given by [16, Eq. (15)] with $N_A = 2$. We further define $\bar{\gamma}_E$ as the average per-antenna SNR at Eve.

We now proceed with the calculation of the secrecy outage probability. Specifically, we rewrite $P_{out}(R_s)$ as

$$P_{out}(R_s) = \underbrace{P_r(C_s < R_s | \gamma_B > \gamma_E) \times P_r(\gamma_B > \gamma_E)}_{V_1} + \underbrace{P_r(\gamma_B < \gamma_E)}_{V_2}, \quad (11)$$

where V_1 is derived as

$$\begin{aligned} V_1 &= \int_0^\infty \int_{\gamma_E}^{2^{R_s}(1+\gamma_E)-1} f_{\gamma_E}(\gamma_E) f_{\gamma_B}(\gamma_B) d\gamma_B d\gamma_E \\ &= \underbrace{\int_0^\infty \int_0^{2^{R_s}(1+\gamma_E)-1} f_{\gamma_E}(\gamma_E) f_{\gamma_B}(\gamma_B) d\gamma_B d\gamma_E}_{U_1} \\ &\quad - \underbrace{\int_0^\infty \int_0^{\gamma_E} f_{\gamma_E}(\gamma_E) f_{\gamma_B}(\gamma_B) d\gamma_B d\gamma_E}_{U_2}. \end{aligned} \quad (12)$$

It is easy to observe that $U_2 = V_2$. As such, we simplify $P_{out}(R_s)$ as $P_{out}(R_s) = U_1$.

To derive U_1 , we first calculate the inner integral with respect to γ_B by substituting $f_{\gamma_B}(\gamma)$ and $f_{\gamma_E}(\gamma)$ into U_1 and applying [17, Eq. (3.351.1)]. We then expand the product of the inner integral and $f_{\gamma_E}(\gamma)$ by applying [17, Eq. (1.111)] and solve the resultant integral with respect to γ_E by applying [17, Eq. (3.351.3)]. By performing some algebraic manipulations, the secrecy outage probability is derived as

$$P_{out}(R_s) = 1 - \frac{N_A(N_A - 1)[\Psi_1 - \Psi_2 + \Psi_3 - \Psi_4]}{[(N_B - 1)!(N_E - 1)!]^2}, \quad (13)$$

$$\Psi_1 = \sum_{i=0}^{N_A-2} \sum_{j=0}^{N_B-1} \sum_{m=0}^{N_E-1} (-1)^{i+1} \mathbb{G} \sum_{t=0}^{(N_B-1)i} a_t(N_B, i) \sum_{k=0}^{\omega_1+k} \left(\frac{2^{R_s} \bar{\gamma}_E}{\bar{\gamma}_B} \right)^{\omega_1} \frac{k! \binom{\omega_1+k}{k}}{2^{\omega_1(i+2)k+1}} e^{-\frac{(2^{R_s}-1)(i+2)}{\bar{\gamma}_B} \sum_{u=0}^{\omega_1} \binom{\omega_1}{u} \left(\frac{2-2^{1-R_s}}{\bar{\gamma}_E} \right)^{\omega_1-u}} \\ \times \left[\sum_{n=0}^{2N_E-m-2} \frac{n! \binom{2N_E-m-2}{n}}{2^{2N_E-m-2}} \mathbf{F}_1(\varphi_1) + \sum_{q=0}^{N_E-m-1} \frac{(-1)^q \binom{N_E-m-1}{q}}{2^{N_E+q-1}(N_E+q)} \mathbf{F}_2(\varphi_1) \right], \quad (13a)$$

$$\Psi_2 = \sum_{j=0}^{N_B-1} \sum_{m=0}^{N_E-1} \mathbb{H} \sum_{p=0}^{N_B-j-1} \frac{(-1)^p \binom{N_B-j-1}{p}}{2^{N_B+p-1}(N_B+p)} \left(\frac{2^{R_s} \bar{\gamma}_E}{\bar{\gamma}_B} \right)^{2N_B-j-1} e^{-\frac{(2^{R_s}+1-2)}{\bar{\gamma}_B} \sum_{u=0}^{2N_B-j-1} \binom{2N_B-j-1}{u} \left(\frac{2-2^{1-R_s}}{\bar{\gamma}_E} \right)^{2N_B-j-u-1}} \\ \times \left[\sum_{n=0}^{2N_E-m-2} \frac{n! \binom{2N_E-m-2}{n}}{2^{2N_E-m-1}} \mathbf{F}_1(\varphi_2) + \sum_{q=0}^{N_E-m-1} \frac{(-1)^q \binom{N_E-m-1}{q}}{2^{N_E+q}(N_E+q)} \mathbf{F}_2(\varphi_2) \right], \quad (13b)$$

$$\Psi_3 = \sum_{i=1}^{N_A-2} \sum_{j=0}^{N_B-1} \sum_{m=0}^{N_E-1} (-1)^i \mathbb{G} \sum_{t=0}^{(N_B-1)i} a_t(N_B, i) \sum_{p=0}^{N_B-j-1} (-1)^p \binom{N_B-j-1}{p} \sum_{k=0}^{\omega_2+k} \frac{k! \binom{\omega_2+k}{k}}{2^{\omega_2 i k+1}} \left(\frac{2^{R_s} \bar{\gamma}_E}{\bar{\gamma}_B} \right)^{\omega_1} e^{-\frac{(2^{R_s}-1)(i+2)}{\bar{\gamma}_B} \sum_{u=0}^{\omega_1} \binom{\omega_1}{u} \left(\frac{2-2^{1-R_s}}{\bar{\gamma}_E} \right)^{\omega_1-u}} \\ \times \sum_{u=0}^{\omega_1} \binom{\omega_1}{u} \left(\frac{2-2^{1-R_s}}{\bar{\gamma}_E} \right)^{\omega_1-u} \left[\sum_{n=0}^{2N_E-m-2} \frac{n! \binom{2N_E-m-2}{n}}{2^{2N_E-m-2}} \mathbf{F}_1(\varphi_1) + \sum_{q=0}^{N_E-m-1} \frac{(-1)^q \binom{N_E-m-1}{q}}{2^{N_E+q-1}(N_E+q)} \mathbf{F}_2(\varphi_1) \right], \quad (13c)$$

$$\Psi_4 = \sum_{i=1}^{N_A-2} \sum_{j=0}^{N_B-1} \sum_{m=0}^{N_E-1} (-1)^{i+1} \mathbb{G} \sum_{t=0}^{(N_B-1)i} a_t(N_B, i) \sum_{p=0}^{N_B-j-1} \frac{(-1)^p \binom{N_B-j-1}{p} (N_B+p+t-1)!}{i^{N_B+p+t}} \left(\frac{2^{R_s} \bar{\gamma}_E}{\bar{\gamma}_B} \right)^{\omega_3} e^{-\frac{(2^{R_s}+1-2)}{\bar{\gamma}_B} \sum_{u=0}^{\omega_3} \binom{\omega_3}{u} \left(\frac{2-2^{1-R_s}}{\bar{\gamma}_E} \right)^{\omega_3-u}} \\ \times \sum_{u=0}^{\omega_3} \binom{\omega_3}{u} \left(\frac{2-2^{1-R_s}}{\bar{\gamma}_E} \right)^{\omega_3-u} \left[\sum_{n=0}^{2N_E-m-2} \frac{n! \binom{2N_E-m-2}{n}}{2^{2N_E-m-2}} \mathbf{F}_1(\varphi_2) + \sum_{q=0}^{N_E-m-1} \frac{(-1)^q \binom{N_E-m-1}{q}}{2^{N_E+q-1}(N_E+q)} \mathbf{F}_2(\varphi_2) \right]. \quad (13d)$$

where Ψ_1, Ψ_2, Ψ_3 and Ψ_4 are presented in (13a), (13b), (13c) and (13d), respectively. In (13a), (13b), (13c) and (13d), we define variables $\omega_1 = 2N_B + t - j - k - 2$, $\omega_2 = N_B + p + t - 1$, $\omega_3 = N_B - j - p - 1$, $\lambda = 2N_E + u - m - n - 3$, $\varphi_1 = \frac{\bar{\gamma}_B + 2^{R_s-1}(i+2)\bar{\gamma}_E}{\bar{\gamma}_B}$, and $\varphi_2 = \frac{\bar{\gamma}_B + 2^{R_s}\bar{\gamma}_E}{\bar{\gamma}_B}$. We also define the functions

$$\mathbb{G} = \binom{N_A-2}{i} j! \binom{N_B-1}{j} m! \binom{N_E-1}{m},$$

$$\mathbb{H} = j! \binom{N_B-1}{j} m! \binom{N_E-1}{m},$$

$$\mathbf{F}_1(\varphi) = (2N_E - m - n - 2) \mathbf{W}(\lambda, \varphi) - \mathbf{W}(\lambda + 1, \varphi),$$

and

$$\mathbf{F}_2(\varphi) = (2N_E - m - 2) \mathbf{W}(\lambda, \varphi) - \mathbf{W}(\lambda + 1, \varphi).$$

We further define $a_t(N_B, i)$ as the coefficients of z^t for $0 \leq t \leq i(N_B - 1)$, which arises from the expansion of

$$\left(\sum_{k=0}^{N_B-1} \frac{z^k}{k!} \right)^i, \quad (14)$$

and define $\mathbf{W}(r, u)$ for $u > 0$ in $\mathbf{F}_1(\varphi)$ and $\mathbf{F}_2(\varphi)$ as

$$\mathbf{W}(r, u) = \int_0^\infty x^r e^{-ux} dx = \begin{cases} r! u^{-r-1}, & \text{if } r = 0, 1, 2, \dots \\ 0, & \text{if } r = -1. \end{cases} \quad (15)$$

It is highlighted that our new expression in (13) is in closed form as it involves finite summations of exponential functions and power functions.

B. Probability of Non-zero Secrecy Capacity

The probability of non-zero secrecy capacity is defined as the probability by which the secrecy capacity is larger than zero. As such, it is expressed as

$$\Pr(C_s > 0) = \Pr(\gamma_B > \gamma_E) = \int_0^\infty \int_0^{\gamma_B} f_{\gamma_B}(\gamma_B) f_{\gamma_E}(\gamma_E) d\gamma_E d\gamma_B. \quad (16)$$

Substituting $f_{\gamma_B}(\gamma)$ and $f_{\gamma_E}(\gamma)$ into (16) and solving the resultant integrals, the explicit expression for $\Pr(C_s > 0)$ is obtained. Due to page limits, the explicit expression is omitted here. Instead, we present $\Pr(C_s > 0)$ in terms of the secrecy outage probability as

$$\Pr(C_s > 0) = 1 - P_{out}(0). \quad (17)$$

C. ε -Outage Secrecy Capacity

The ε -outage secrecy capacity is defined as the maximum secrecy rate for which the secrecy outage probability is no larger than ε . Specifically, it is characterized as

$$C_{out}(\varepsilon) = \underset{P_{out}(R_s) \leq \varepsilon}{\operatorname{argmax}} R_s. \quad (18)$$

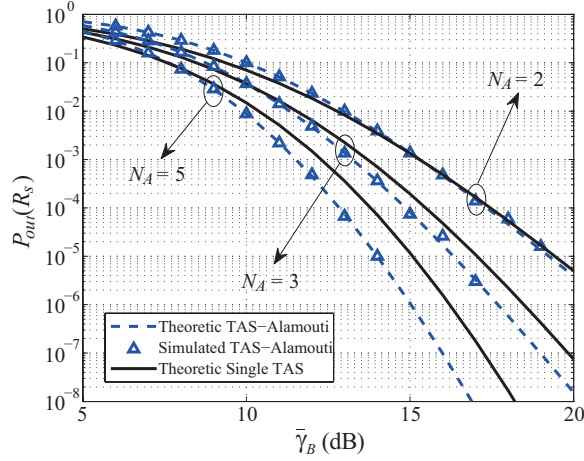


Fig. 2. Secrecy outage probability versus $\bar{\gamma}_B$ for $R_s = 1$, $\bar{\gamma}_E = 5$ dB, $N_B = 3$, and $N_E = 2$.

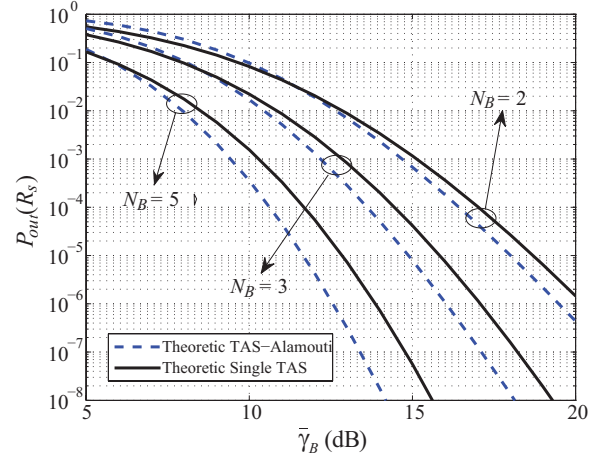


Fig. 3. Secrecy outage probability versus $\bar{\gamma}_B$ for $R_s = 1$, $\bar{\gamma}_E = 5$ dB, $N_A = 4$, and $N_E = 2$.

Substituting (13) into (18) and applying numerical root finding, $C_{out}(\varepsilon)$ is obtained.

IV. NUMERICAL RESULTS

In this section, we present numerical results to examine the impact of the number of antennas and the average SNRs on the secrecy performance. Specifically, we conduct a thorough performance comparison between our TAS-Alamouti scheme with the single TAS scheme in [12]. This comparison highlights the potential of TAS-Alamouti.

We first examine the impact of N_A on the secrecy outage probability. Fig. 2 plots $P_{out}(R_s)$ versus $\bar{\gamma}_B$ for different N_A . In this figure, the theoretical TAS-Alamouti curve is generated from (13), and the theoretical single TAS curve is generated from [12, Eq. (13)]. We first observe that $P_{out}(R_s)$ of TAS-Alamouti significantly decreases as N_A increases. Moreover, we observe that TAS-Alamouti achieves a lower $P_{out}(R_s)$ than single TAS when $\bar{\gamma}_B$ is in the medium and high regime. For example, TAS-Alamouti outperforms single TAS when $\bar{\gamma}_B > 10$ dB for $N_A = 3$. This is due to the fact that more transmit energy is wasted on the second strongest antenna for Eve than for Bob at medium and high $\bar{\gamma}_B$. Furthermore, we observe that TAS-Alamouti provides a higher $P_{out}(R_s)$ than single TAS when $\bar{\gamma}_B$ is low. As such, it is easy to determine the crossover point at which TAS-Alamouti and single TAS achieve the same performance. Notably, we find that the value of $\bar{\gamma}_B$ at the crossover point decreases as N_A increases. This can be explained by the fact that the two selected transmit antennas are determined by Bob and the freedom of α increases with N_A . Finally, we observe that the theoretical curves match precisely with the Monte Carlo simulations. This verifies the correctness of our analysis. Monte Carlo simulations are omitted in other figures to avoid cluttering.

We next examine the impact of N_B and N_E on the secrecy outage probability. Fig. 3 plots $P_{out}(R_s)$ versus $\bar{\gamma}_B$ for

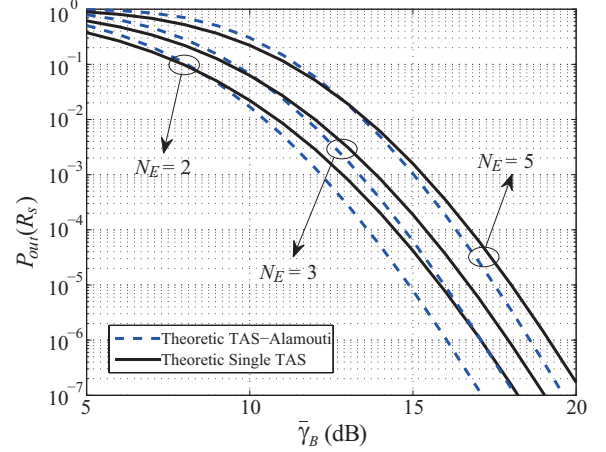


Fig. 4. The secrecy outage probability versus $\bar{\gamma}_B$ for $R_s = 1$, $\bar{\gamma}_E = 5$ dB, $N_A = 4$, and $N_B = 3$.

different N_B . In this figure, we observe that $P_{out}(R_s)$ of TAS-Alamouti profoundly decreases as N_B increases. Moreover, we observe that the value of $\bar{\gamma}_B$ at the crossover point decreases as N_B increases. This is due to the fact that larger N_B increases the freedom of \mathbf{f}_α . Fig. 4 plots $P_{out}(R_s)$ versus $\bar{\gamma}_B$ for different N_E . In this figure, we observe that $P_{out}(R_s)$ of TAS-Alamouti increases as N_E increases. In addition, we observe that the value of $\bar{\gamma}_B$ at the crossover point increases as N_E increases. This arises from the fact that larger N_E increases the freedom of \mathbf{g}_α .

We now focus our attention on the probability of non-zero secrecy capacity. Fig. 5 plots $P_{out}(R_s)$ versus $\bar{\gamma}_B$ for different $\bar{\gamma}_E$. In this figure, the theoretical TAS-Alamouti curve is generated from (16), and the theoretical single TAS curve is generated from [12, Eq. (29)]. From Fig. 5, we see that the $\Pr(C_s > 0)$ of TAS-Alamouti is higher than that of single TAS when $\bar{\gamma}_B$ is larger than a specific value. In particular, we observe that the value of $\bar{\gamma}_B$ at the crossover point is

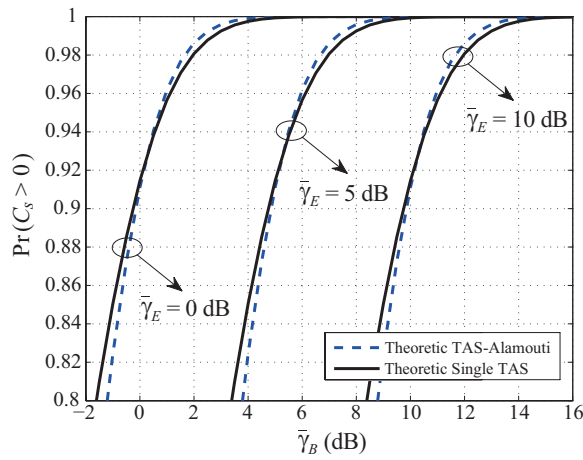


Fig. 5. The probability of non-zero secrecy capacity versus $\bar{\gamma}_B$ for $N_A = 4$, $N_B = 3$, and $N_E = 2$.

around $\bar{\gamma}_E$. Notably, this value increases as $\bar{\gamma}_E$ increases. Additionally, we observe that $\Pr(C_s > 0)$ of TAS-Alamouti still exists when $\bar{\gamma}_B < \bar{\gamma}_E$.

Finally, we examine the ε -outage secrecy capacity. Fig. 6 plots $C_{out}(\varepsilon)$ versus N_A for different N_E . In this figure, the theoretical TAS-Alamouti curve is generated from (18), and the theoretical single TAS curve is generated from [12, Eq. (31)]. From this figure, we see that $C_{out}(\varepsilon)$ of TAS-Alamouti increases with N_A but decreases with N_E . We also see that TAS-Alamouti achieves a higher $C_{out}(\varepsilon)$ than single TAS when N_A is larger than a certain value.

V. CONCLUSION

In this work we have introduced a new TAS-Alamouti scheme for physical layer security enhancement in MIMO wiretap channels. Adopting non-identical Rayleigh fading between the main channel and the eavesdropper's channel, we derived a new closed-form expression for the secrecy outage probability, based on which the probability of non-zero secrecy capacity and ε -outage secrecy capacity were characterized. We proved that the our TAS-Alamouti scheme achieves lower secrecy outage probability than the single TAS scheme when the SNR of the main channel is in the medium and high regime relative to the SNR of the eavesdropper's channel. Future directions for our new scheme include its integration with location verification techniques [18] [19] for even more enhanced security at the wireless physical layer.

ACKNOWLEDGMENTS

This work was funded by The University of New South Wales and Australian Research Council Grant DP120102607.

REFERENCES

- [1] Y.-S. Shiu, S. Y. Chang, H.-C. Wu, S. C.-H. Huang, and H.-H. Chen, "Physical layer security in wireless networks: A tutorial," *IEEE Commun. Mag.*, vol. 18, no. 5, pp. 66–74, Apr. 2011.
- [2] H. V. Poor, "Information and inference in the wireless physical layer," *IEEE Commun. Mag.*, vol. 19, no. 1, pp. 40–47, Feb. 2012.

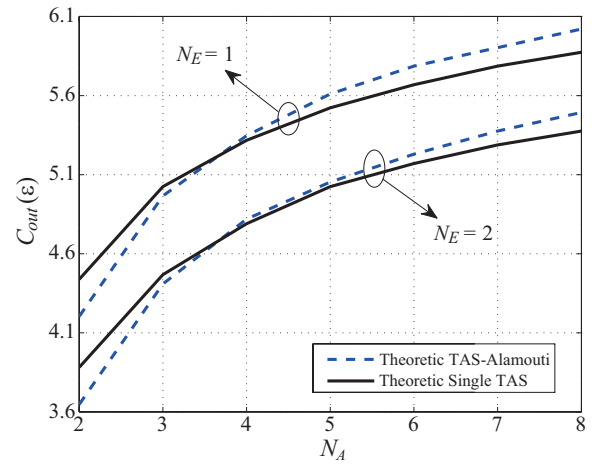


Fig. 6. The ε -outage secrecy capacity versus N_A for $\varepsilon = 0.01$, $\bar{\gamma}_B = 20$ dB, $\bar{\gamma}_E = 0$ dB, and $N_B = 2$.

- [3] C. E. Shannon, "Communication theory of secrecy systems," *Bell Syst. Techn. J.*, vol. 28, no. 4, pp. 656–715, Oct. 1949.
- [4] A. Wyner, "The wire-tap channel," *Bell Syst. Techn. J.*, vol. 54, no. 8, pp. 1355–1387, Oct. 1975.
- [5] S. K. Leung-Yan-Cheong and M. E. Hellman, "The Gaussian wire-tap channel," *IEEE Trans. Inf. Theory*, vol. 24, no. 4, pp. 451–456, Jul. 1978.
- [6] A. Khisti and G. W. Wornell, "Secure transmission with multiple antennas—Part II: The MIMOME wiretap channel," *IEEE Trans. Inf. Theory*, vol. 56, no. 11, pp. 5515–5532, Nov. 2010.
- [7] F. Oggier and B. Hassibi, "The secrecy capacity of the MIMO wiretap channel," *IEEE Trans. Inf. Theory*, vol. 57, no. 8, pp. 4961–4972, Aug. 2011.
- [8] S. Goel and R. Negi, "Guaranteeing secrecy using artificial noise," *IEEE Trans. Wireless Commun.*, vol. 7, no. 6, pp. 2180–2189, Jun. 2008.
- [9] A. Mukherjee and A. L. Swindlehurst, "Robust beamforming for secrecy in MIMO wiretap channels with imperfect CSI," *IEEE Trans. Signal Process.*, vol. 59, no. 1, pp. 351–361, Jan. 2011.
- [10] M. Bloch, J. Barros, M. Rodrigues, and S. McLaughlin, "Wireless information-theoretic security," *IEEE Trans. Inf. Theory*, vol. 54, no. 6, pp. 2515–2534, Jun. 2008.
- [11] H. Alves, R. D. Souza, M. Debbah, and M. Bennis, "Performance of transmit antenna selection physical layer security schemes," *IEEE Signal Process. Lett.*, vol. 19, no. 6, pp. 372–375, Jun. 2012.
- [12] N. Yang, P. L. Yeoh, M. El-Kashlan, R. Schober, and I. B. Collings, "Secure transmission via transmit antenna selection in MIMO wiretap channels," in *Proc. IEEE Globecom*, Anaheim, CA, Dec. 2012, pp. 807–812.
- [13] N. Yang, P. L. Yeoh, M. El-Kashlan, R. Schober, and I. B. Collings, "Transmit antenna selection for security enhancement in MIMO wiretap channels," *IEEE Trans. Commun.*, vol. 61, no. 1, pp. 144–154, Jan. 2013.
- [14] J. Yuan, "Adaptive transmit antenna selection with pragmatic space-time trellis codes," *IEEE Trans. Wireless Commun.*, vol. 5, no. 7, pp. 1706–1715, Jul. 2006.
- [15] S. Alamouti, "A simple transmit diversity technique for wireless communications," *IEEE J. Sel. Areas Commun.*, vol. 16, no. 8, pp. 1451–1458, Oct. 1998.
- [16] Z. Chen, J. Yuan, B. Vucetic, and Z. Zhou, "Performance of Alamouti scheme with transmit antenna selection," *Electron. Lett.*, vol. 39, pp. 1666–1668, Nov. 2003.
- [17] I. S. Gradshteyn and I. M. Ryzhik, *Table of Integrals, Series and Products*, 7th ed., Academic, San Diego, CA, 2007.
- [18] R. A. Malaney, "Securing Wi-Fi networks with position verification: extended version," *International J. Security Netw.*, vol. 2, pp. 27–36, Mar. 2007.
- [19] S. Yan, R. Malaney, I. Nevat, and G. Peters, "An information theoretic location verification system for wireless networks," in *Proc. IEEE Globecom*, Anaheim, CA, Dec. 2012, pp. 5637–5642.